Journal of Earthquake Engineering

ISSN: (Print) (Online) Journal homepage: www.tandfonline.com/journals/ueqe20

Seismic Scenario Losses Estimation Based on the Vulnerability of Pre-Code Masonry Buildings in the Metropolitan Area of Lisbon

V. Bernardo, A. Campos Costa, P. Candeias, A. R. Carvalho & A. Costa

JOURNAL OF EARTHQUAKE ENGINEERING
https://doi.org/10.1080/13632469.2024.2379396

Seismic Scenario Losses Estimation Based on the Vulnerability of Pre-Code Masonry Buildings in the Metropolitan Area of Lisbon

V. Bernardo [a], A. Campos Costa [a], P. Candeias [a], A. R. Carvalho [a], and A. Costa [b]

[a]Earthquake Engineering and Structural Dynamics Unit (Structures Department), National Laboratory for Civil Engineering, Lisbon, Portugal; [b]Department of Civil Engineering, University of Aveiro, Aveiro, Portugal

ABSTRACT

The metropolitan area of Lisbon is the region of Portugal with the highest seismic risk, given the coexistence of moderate-to-high hazard with high population density and building stock exposure. The present work addresses the seismic risk assessment of pre-code masonry buildings in this region, accounting various typological classes and conservation states in order to evaluate the consequences in terms of economic losses. The analyses are conducted through a seismic probabilistic approach, considering the site-specific ground motion through a non-stationary stochastic method. The results can serve as a useful guide for decision-making in developing regional seismic risk mitigation strategies.

ARTICLE HISTORY
Received 29 August 2022
Accepted 8 July 2024

KEYWORDS
Seismic risk analysis; metropolitan area of Lisbon; pre-code masonry building; seismic probabilistic approach; seismic vulnerability assessment

1. Introduction

The metropolitan area of Lisbon (MAL) is composed by 18 municipalities and 211 parishes, with a total area of 2,957.5 km^2 and a population density of around 950 people/km^2 (INE 2012). The MAL has the highest population and building density in Portugal, contributing approximately 34% to the country's GDP (2020). Located on the Eurasian plate in the vicinity of the southern boundary with the African plate, Lisbon is susceptible to high offshore earthquakes and moderate-to-high onshore earthquakes (Vilanova and Fonseca 2007). Approximately 35% of the building stock in Lisbon consists of masonry buildings, which are often susceptible to earthquake ground motions even during moderate events (Costa et al. 2010; Vicente et al. 2011). Furthermore, most of these buildings were only designed to withstand gravity loads as the First Code for Building Safety Against Earthquakes (RSCCS 1958) was only introduced in 1958.

Over the past centuries, several earthquakes have affected the region of Lisbon, influencing the local seismic building culture (Correia, Lourenço, and Varum 2015; Pereira and Romao 2016), including the well-known 1755 Lisbon offshore earthquake (Mw = 8.5–9.0) and subsequent tsunami and fires that devastated downtown Lisbon; the 1909 Benavente earthquake (Mw = 6.3), which remains the largest onshore earthquake that occurred in the Iberian Peninsula (Tagus Valley, approximately 60 km northeast from Lisbon), resulting in around 46 fatalities and serious damage to 879 buildings, particularly in masonry constructions, as reported in (Choffat and Bensaúde 1912). Other relevant seismic events affected the country, causing death and destruction, particularly in the south of Portugal and Setubal (Pereira and Romao 2016).

In the last decades, several seismic risk studies have been carried out at various scales, driven by a growing public awareness of the importance of safeguarding human life and architectural heritage: at a global scale, it highlighted the research developed by the Global Earthquake Model Foundation

CONTACT V. Bernardo vbernardo@lnec.pt; vms.bernardo@gmail.com; vbernardo@civil.uminho.pt Earthquake Engineering and Structural Dynamics Unit (Structures Department), National Laboratory for Civil Engineering, Av. do Brasil 101, Lisbon 1700-075, Portugal

(GEM) (Crowley et al. 2013; Silva et al. 2018). In Europe, the research project RISK-UE (Mouroux and Le Brun 2006), LESSLOSS (Flesch 2007), PERPETUATE (Lagomarsino and Cattari 2015) and ESRM20 (Crowley et al. 2021). Other studies can be found in the literature providing tools for seismic risk analysis (e.g. Battegazzorre et al. 2021; De Iuliis et al. 2023; Domaneschi et al. 2021; Domaneschi, Cimellaro, and Scutiero 2019; Marasco, Cardoni, et al. 2021; Marasco, Noori, et al. 2021; Marasco, Zamani Noori, et al. 2021). The seismic risk in Portugal was evaluated in 2006 by Sousa (2006a) and in 2014 by Silva et al. (2014). In the latter, an economic toll of 15.7% (approximately 56,000 M €) of the Portuguese residential building stock value has been estimated for a return period of 475 years (Silva et al. 2014). Both studies report MAL as the region of Portugal with the highest seismic risk, given the coexistence of a moderate-to-high seismic hazard, high population density, and a high building stock exposure. In particular, the seismic risk assessment of Lisbon was investigated by Sousa, Campos Costa, and Caldeira (2010) considering various seismic scenarios, concluding that the risk is higher in Lisbon's city center (Old Lisbon) for a short distance seismic scenario. Campos Costa et al. (2010) evaluated the seismic risk and mitigation strategies for the existing building stock in the MAL region, concluding that economic losses vary from 1.3% to 38% for 95- and 5000-years return period, respectively; furthermore, approximately 36% of the total economic risk corresponds to masonry buildings. Tang et al. (2012) evaluated the seismic risk in the MAL region under the occurrence of the 1755 earthquake and subsequent tsunami, reporting that seismic mitigation measures and emergency plans are needed for downtown Lisbon. Other research works at urban scale have been carried out in Portugal and can be found in literature, e.g. Coimbra (Vicente et al. 2011), Faro (Vicente, Ferreira, and Maio 2014) and Seixal (Ferreira et al. 2013). It is important to emphasize that most of the aforementioned studies were essentially based on expert judgment or empirical models to characterize the seismic vulnerability of the building stock.

In the framework of the present study, the expected economic losses in the MAL region for the Lower Tagus Valley Fault (LTVF), which is the worst seismic scenario for the MAL region (Sousa 2006a), were evaluated through a seismic probabilistic approach, identifying the parishes with the highest risk. The study relies on a synthetic database of 18.000 building representative of the main geometrical and mechanical features of pre-code masonry buildings with a large scatter of material properties to take into account the variability in the building stock (Bernardo, Campos Costa, et al. 2021). The seismic performance of the structures was computed for the LTVF considering 150 stochastic realizations per each Mw, in order to account for the uncertainty in the synthesis of ground motions due to seismic fault rupturing, wave propagation, and site effects. Finally, the vulnerability curves were derived considering both uncertainties in the building's capacity and response.

2. Methodology for Seismic Risk Analysis: Review

Seismic risk assessment is crucial for guiding decision-making, urban planning, and disaster risk reduction initiatives aimed at minimizing the impact of earthquakes on community.

The term seismic risk can be defined by the convolution of seismic hazard, vulnerability, and exposure. The seismic risk of a given location aims to estimate the expected losses incurred by exposed elements during future seismic events and the likelihood of such events occurring, i.e. seismic hazard, within a given investigation time. In this context, the elements exposed (e.g. building, group of buildings or infrastructures, cities, population) are characterized by their susceptibility to damage by the ground shaking during an earthquake, i.e. seismic vulnerability. The variation of each of these three components (hazard, vulnerability, and exposure) influences the severity of the seismic risk level. For instance, the increase in population and its concentration in earthquake-prone old urban centers, such as downtown Lisbon, have increased the level of seismic risk in recent years.

Over the last decades, several approaches for seismic risk assessment have been proposed based on numerical and/or empirical models (e.g. D'Ayala 2013; Foerster et al. 2009; Martins and Silva 2021). In the present study, a seismic probabilistic approach based on numerical models is used, which can be mathematically described by the following Eq. (1) (e.g. McGuire 2004; Sousa 2006a) and schematized

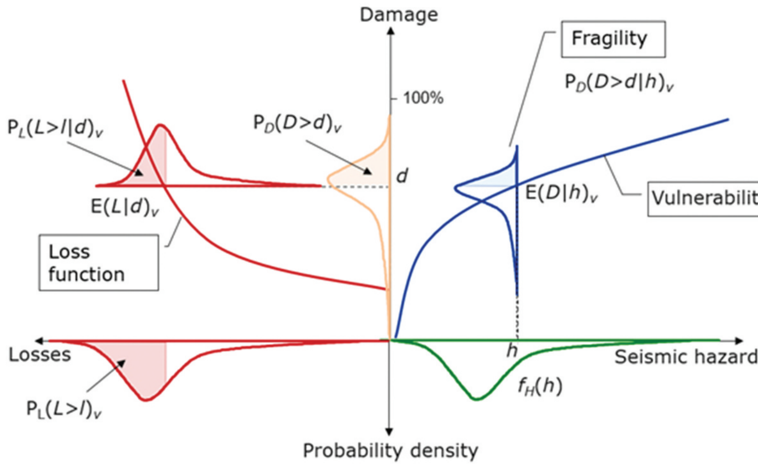

Figure 1. Generic scheme of the probabilistic seismic risk modelling for a given structure with vulnerability v (adapted from Sousa, Campos Costa, and Caldeira 2010).

in Fig. 1 (adapted from Sousa, Campos Costa, and Caldeira 2010), assuming a given structure with vulnerability v.

$$P(L>l) = \int_D \int_H P(L>l|d)P(D>d|h)f_H(h)\mathrm{d}h\,\mathrm{d}d \tag{1}$$

where, $f_H(h)$ is the probability density function of the seismic hazard h; $P(D>d|h)$ the probability distribution of the damage variable d conditioned by a certain level of seismic hazard, i.e. the seismic fragility; $P(L>l|d)$ the probability distribution of losses l conditioned by a given damage d. Since this last distribution cannot be obtained directly, the estimation of economic losses due to physical damages is usually associated to the damage state d through a damage ratio DR_d (Hill and Rossetto 2008) defined by the repair cost to the replacement cost (Rojahn et al. 1985). The conversion of damage states into repair/replacement costs results in a loss index that defines an expected loss value conditioned by a given seismic hazard $E(L|h)$, which can be estimated by the weighted average of the number of buildings in a particular damage state by DR_d (Costa et al. 2010). Finally, the economic expected losses conditioned by a seismic hazard h are computed from the product of $E(L|h)$ by the replacement cost of the building.

3. Building Stock Characterization: Geometry and Economic Exposure

The metropolitan area of Lisbon (MAL), Fig. 2, is composed of 434,600 residential buildings and 1,423,654 dwellings (INE 2012), where masonry buildings represent around 35%. The building stock

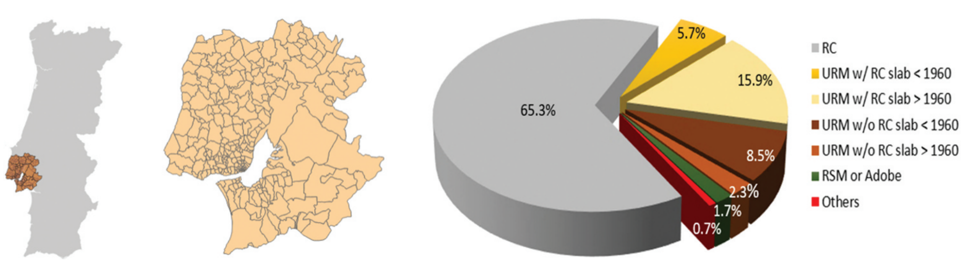

Figure 2. Geographic location of the MAL region (left) and distribution of the building stock (right).

Table 1. Statistical properties for the geometric parameters (Bernardo, Campos Costa, et al. 2021).

Moments	L_x [m]	L_y [m]	IWD [-]	H_0 [m]	H_n [m]	OR_F [-]	OR_B [-]	Th_1 [m]	Th_2 [m]	Th_3 [m]	Th_4 [m]	AWTR [-]
Mean μ	12.6	12.1	0.054	3.23	3.01	0.23	0.21	0.47	0.34	0.21	0.14	0.11
Std. deviation σ	5.00	4.1	0.01	0.42	0.24	0.08	0.08	0.14	0.11	0.05	0.02	0.06

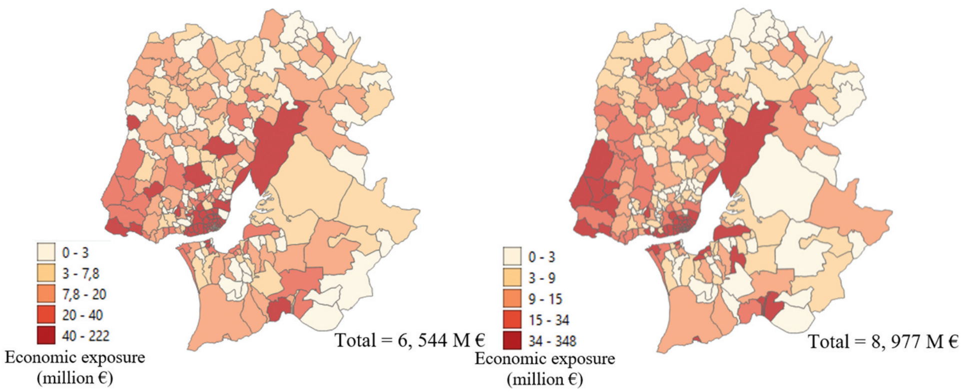

Figure 3. Replacement costs for masonry buildings with rigid (left) and flexible (right) floors in the MAL region.

considered for the risk analysis corresponds to residential pre-code masonry buildings built before the enforcement of the first seismic code in 1958 (RSCCS 1958). The vast majority of these buildings are up to five stories high (INE 2012). Figure 2 shows the disaggregation of the building stock by typology in this region. A detailed summary of the main features of the pre-code masonry buildings and its disaggregation in terms of period of construction and number of floors is presented in Bernardo, Campos Costa, et al. (2021).

The definition of representative building layouts for the subsequent analysis was based on the statistical information collected by Bernardo, Campos Costa, et al. (2021). This study provided the statistical properties for the geometric parameters obtained from dozens of original blueprints consulted in the municipal archives. The summary of these properties is presented in Table 1: plan dimensions – L_x and L_y; ground and upper floor stories high – H_0 and H_n; opening ratio – *OR*: front (*ORF*) and back (*ORB*) facade; interior wall density – *IWD*; wall thickness *Th*: facades (1), lateral (2), interior (3), partitions (4); average wall thickness reduction on the façade – *AWR*. This information was used to build representative archetypes of the pre-code masonry building stock and derive the corresponding vulnerability functions (see next section).

Taking into account the statistics provided in Bernardo, Campos Costa, et al. (2021), the average floor areas of pre-code masonry building are around 50 m^2, 100 m^2, 150 m^2, 200 m^2, and 250 m^2 for one to five stories high, respectively. Considering the average cost of repairing and replacing in 2020 equal to 828.48 €/m^2, a total amount of 15,521 M € was estimated for the pre-code masonry building stock in the MAL region, which corresponds to approximately 6.7% of the GDP (2020). Figure 3 shows the replacement cost maps disaggregated by parishes for buildings with RC slabs and timber floors, assigned to rigid and flexible floor diaphragms, respectively.

4. Definition of Seismic Scenarios for Risk Analysis

The seismic action considered for the subsequent analysis is based on the scenario corresponding to the onshore source area of Lower Tagus Valley Fault (LTVF), which is the worst scenario for the MAL region according to the results presented in Bernardo et al. (2022) and as discussed by Sousa (2006a).

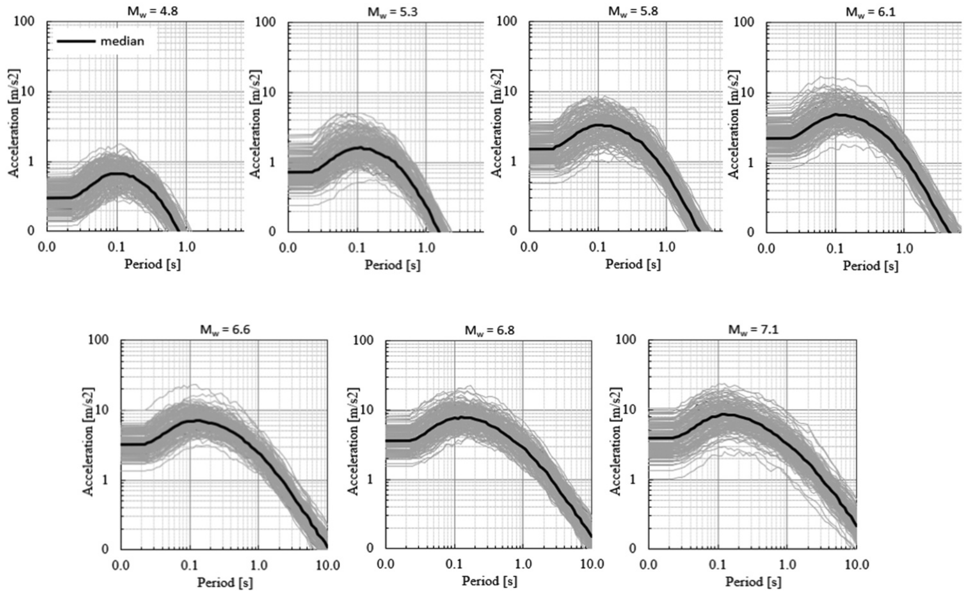

Figure 4. Acceleration response spectra at bedrock for LTVF scenario and different magnitudes.

The seismic ground motions were simulated by means of a seismological numerical model based on a non-stationary stochastic finite-fault method developed at LNEC (Carvalho et al. 2008). For a given seismic zone generation, the non-stationary stochastic method used for the series generation is based on the research assumptions of Beresnev and Atkinson (1998) and adapted for Portugal (Carvalho et al. 2008; Costa et al. 2010). The finite-earthquake-source modelling technique includes a fault discretized into several elements (sub-faults), a nucleation point (initial rupture point), a heterogeneous slip distribution, a rupture velocity, and the sum, at the target site, of the contribution of each element lagged in time. The ground motion at an observation point is thus obtained by summing the contributions from all sub-faults. The characteristics of a fault rupture as a large finite source, including rupture propagation, directivity effects, and source geometry, can profoundly influence the amplitude, frequency content, and duration of a ground motion. To address uncertainties in synthesizing ground motions resulting from seismic fault rupturing and wave propagation, 150 stochastic realizations were generated for each Mw. The pair magnitude distance associated with a given return period is the modal values (most representatives) resulting from a previous disaggregation hazard study (Campos Costa et al. 2006). Figure 4 depicts the acceleration response spectra for 150 simulations performed for each seismic scenario at bedrock, considering the following range of return periods, Tr-years, and the corresponding moment magnitude Mw (in parenthesis): 20 (4.8), 50 (5.3), 100 (5.8), 275 (6.1), 475 (6.6), 1100 (6.8), and 2500 (7.1). It is important to note that, although site effects are not taken into account, the percentage of buildings in the MAL region located on hard soils is around 60% (Costa et al. 2010; INE 2012).

5. Seismic Vulnerability Assessment

Vulnerability functions were derived considering the seismic scenario defined in the previous section. For this purpose, the study relies on a previous comprehensive work conducted through intensive nonlinear static analyses and carried out by the authors (Bernardo, Campos Costa, et al. 2021). This includes different classes of buildings (archetypes) represented with multiple index buildings based on Monte Carlo simulations in which pre-defined statistics on geometrical and material characteristics were considered, resulting in a synthetic database of a total of 18.000 buildings. Regarding material properties, two main classes of typologies were considered to cover the wide range found in the literature review (Candeias et al. 2020): *Type I* – buildings with good-quality masonry (e.g. regular and squared masonry, brick masonry with cement lime mortar) or in a good state of conservation; *Type II* – buildings with poor-quality masonry (e.g. rubble stone masonry, brick masonry with lime mortar) or in a poor state of conservation. The characterization of random variables for masonry mechanical properties is defined in (Bernardo, Sousa, et al. 2021). Finally, different types of floors were also analyzed, including rigid (Milosevic 2019) and flexible (A. G. G. Simões 2018) floor diaphragms.

5.1. Seismic Performance of the Buildings

Considering the capacity curves derived for the entire synthetic database (Bernardo, Campos Costa, et al. 2021), the median curves are presented in Fig. 5 by considering archetypes grouped with equal probability, i.e. the geometry variable was equally weighted and stratified by the numbers of stories (1 to 5), typology (Type I and Type II), and floor diaphragm (rigid and flexible). Structural models for nonlinear analyses were developed using the equivalent frame modeling approach (Penna, Lagomarsino, and Galasco 2014) implemented in the research version of TreMuri software, where only the in-plane behavior is considered.

The limit states depicted in Fig. 5 were also defined according to Bernardo, Sousa, et al. (2021), namely the Damage Limitation – DL, Significant Damage – SD, and Near Collapse – NC. The dispersion in the capacity β_C was evaluated in terms of interstorey drift, i.e. maximum drift in the building, and includes the variability in the randomness of the material

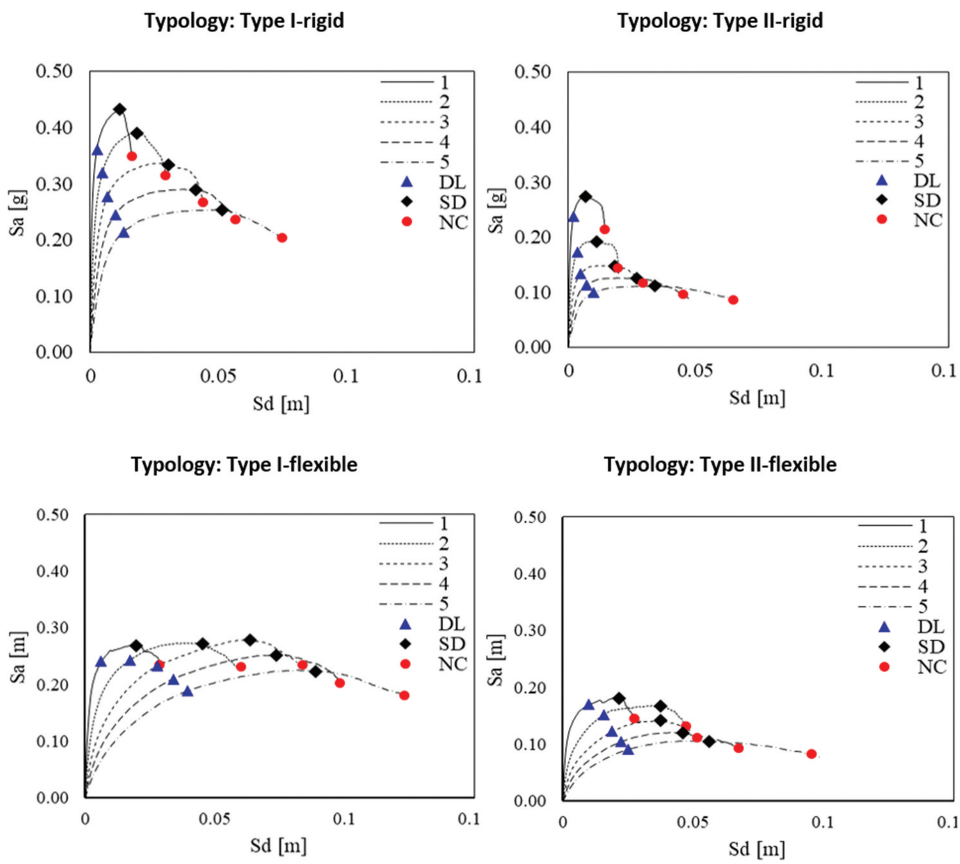

Figure 5. Median capacity curves of the buildings up to five stories high and limit states definition.

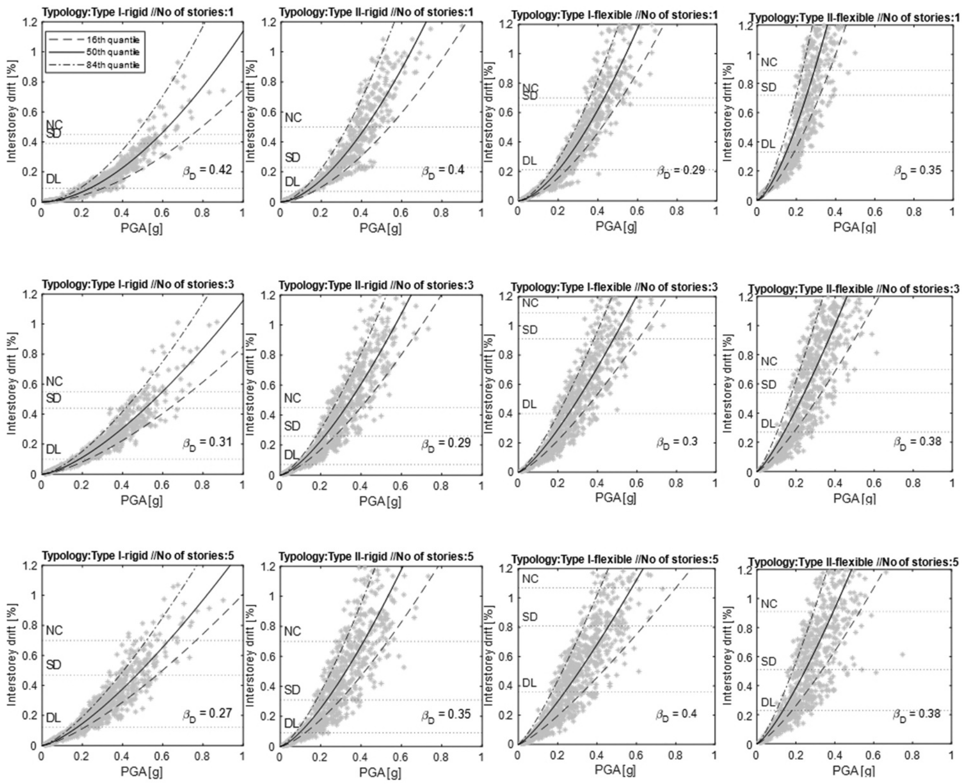

Figure 6. Relationship between the interstory drift (EDP) and PGA (IM); variability in the seismic demand β_D; definition of the limit states adopted in terms of PGA: DL (damage limitation), SD (significant damage), near collapse (NC).

properties and the various archetypes layouts, ranging from: Type I/rigid – 0.30 to 0.33 (DL), 0.12 to 0.26 (SD), 0.15 to 0.32 (NC); Type II/rigid – 0.41 to 0.51 (DL), 0.50 to 0.58 (SD), 0.20 to 0.50 (NC); Type I/flexible – 0.20 to 0.40 (DL), 0.19 to 0.30 (SD), 0.22 to 0.33 (NC); Type II/flexible – 0.27 to 0.62 (DL), 0.34 to 0.60 (SD), 0.30 to 0.50 (NC). Further information regarding the β_C values and the comparison with previous works can be consulted in Bernardo, Sousa, et al. (2021).

The seismic performance of the structures was computed for the previous 150 simulations for each seismic scenario with the capacity curves of Fig. 5 using the improved Capacity Spectrum Method proposed in FEMA 440 (2005). Figure 6 shows the relationship between the performance points (gray dots) in terms of the interstorey drift θ_C as the engineering demand parameter (EDP) and the intensity measure (IM), expressed by the PGA values corresponding to the stochastic realizations of Fig. 4.

The relationship θ_C(EDP) – PGA(IM) was described by an analytical function with a first-order power law fitted to the performance points (gray dots) over the entire range of IM (16th, 50th and 84th quantiles). Based on these results, the adopted limit states defined by the θ_C were expressed in terms of PGA. The dispersion in demand β_D (see Fig. 6) was also computed from the standard deviation of the logarithmic error between the analytical function fitted and the empirical data.

Analyzing the results of Fig. 6, the β_D values in the Type I-rigid typology seem to decrease with the number of stories, while an opposite trend is verified in other typologies, except for one-story buildings. There is also a greater increase in values of interstorey drift for the same value of PGA in Type II typology (low-quality material), in particular for flexible floor diaphragms, as expected.

The selection of PGA as IM will allow to compare the seismic fragility curves derived in the following section with the ones proposed in the literature.

5.2. Derivation of Seismic Fragility Curves

The fragility curves presented in this section represent the probability of exceeding a specific limit state (LS) for a given value of the seismic intensity measure (IM), herein expressed in terms of PGA. The power regressions derived in Fig. 6 were useful to compute the adopted LS in terms of IM, allowing to extract the corresponding PGA values. Figure 7 summarizes these values of PGA for different typologies and number of stories, considering the power function fitted to the median quantile (see Fig. 6) of the data.

The results obtained in the present work were compared with others available in the literature for similar typologies in Lisbon, in particular those presented in Milosevic, Cattari, and Bento (2020) and A. G. Simões et al. (2020) for three stories high buildings (rigid floors) and five stories high buildings (flexible floors), respectively. These studies considered nonlinear static analyses and several ground motions compliant with the EC8 seismic action (onshore scenario). Regarding the results presented in Milosevic, Cattari, and Bento (2020), the values of PGA (g) vary, approximately, between 0.10 and 0.15 (slight), 0.20 and 0.30 (moderate), and 0.30 and 0.40 (extensive and NC), which are in line with the ones proposed in the present study for the Type II typology. Concerning the results obtained in A. G. Simões et al. (2020), the values of PGA(g) vary between 0.08 and 0.12 (slight LS), 0.10 and 0.20 (moderate), 0.30 and 0.40 (extensive), and 0.40 and 0.55 (extensive), which are also in agreement with the values presented in Fig. 7 for typology Type II (five stories high). Note that, the material properties adopted in both previous studies are in the range of the random mechanical properties considered in the present study for type II typology (Bernardo, Campos Costa, et al. 2021).

The total dispersion β_{total} employed in the fragility curves combines through the square-root of the sum of squares (Vamvatsikos 2013) the values of β_D (see previous section) and β_C proposed in

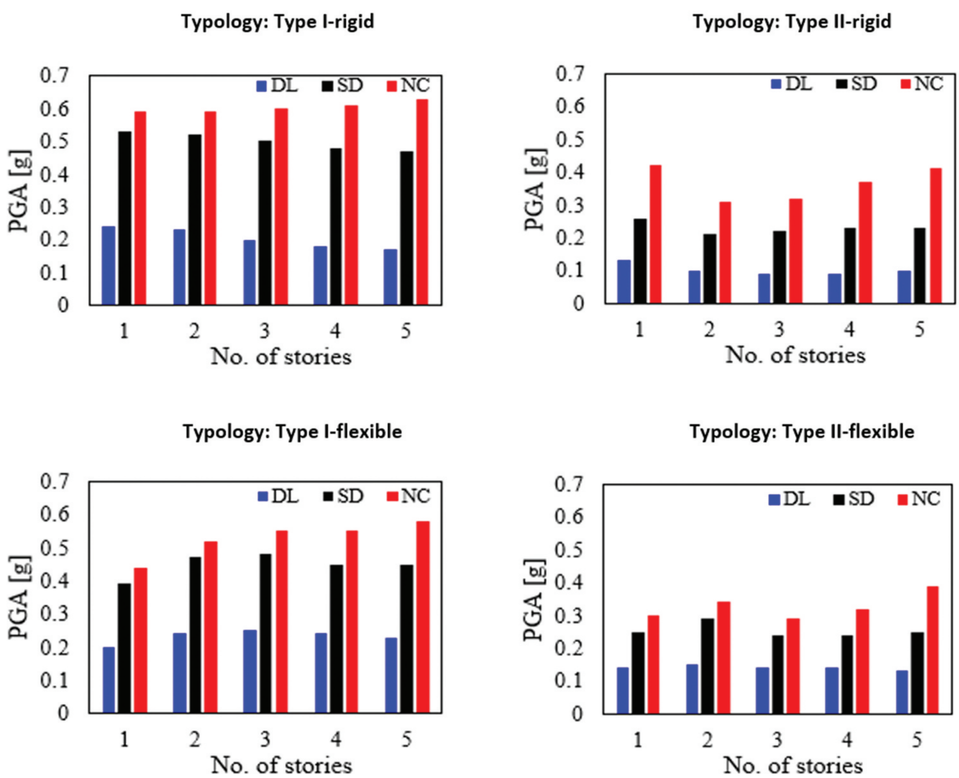

Figure 7. Values of PGA (median quantile) corresponding to the limit state thresholds adopted.

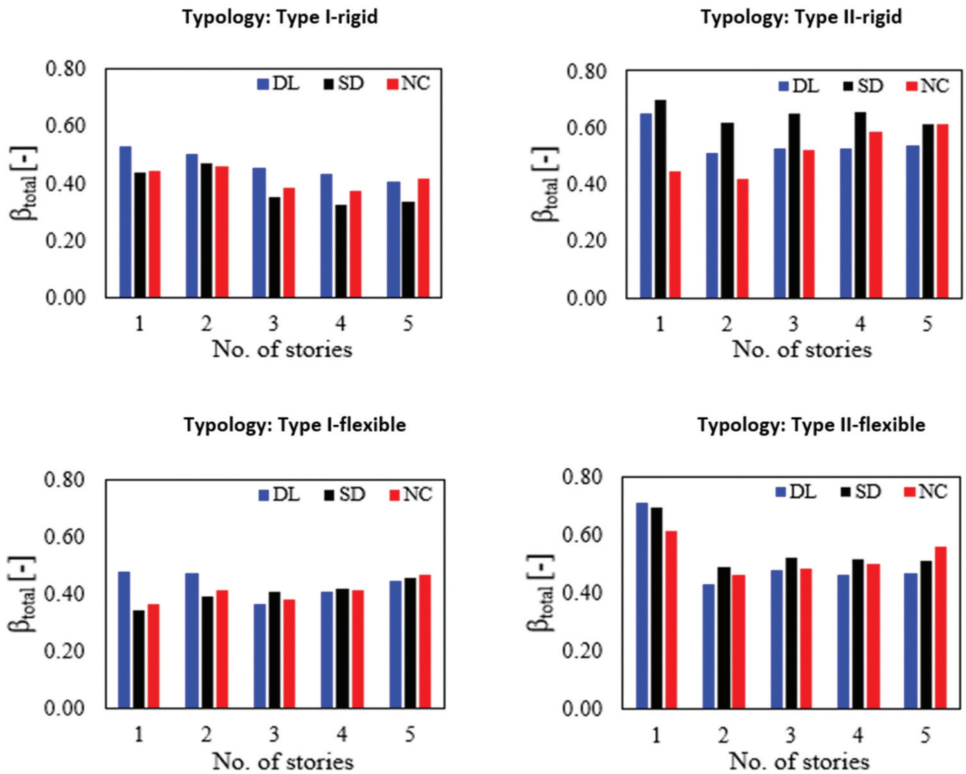

Figure 8. Total dispersion β_{total}.Including the variability in the capacity and seismic demand.

Bernardo et al. 2022. Figure 8 summarizes the values of β_{total} for the different typologies and number of stories.

The values of β_{total} obtained in this study were also compared with the reference values available in the literature: the values proposed by Milosevic, Cattari, and Bento (2020) and A. G. Simões et al. (2020) range between 0.25 to 0.30 and 0.40 to 0.60, respectively. Note that, the values presented by A. G. Simões et al. (2020) are similar to the ones proposed in the present study, since they also account for different prototypes of buildings analyzed. Other authors report values of β_{total}, including the variability in the capacity and seismic demand, in the range of 0.28 to 0.70 (Barbat, Pujades, and Lantada 2008) and 0.37 to 0.80 (Douglas et al. 2015) for URM buildings, which are in line with the values achieved in this study.

Figure 9 presents the seismic fragility curves (16%, 50%, and 84% quantiles) for the different typologies (three and five stories high buildings, rigid and flexible floor diaphragm), considering the analytical cumulative distribution functions proposed in (Bernardo, Campos Costa, et al. 2021). In general, the differences between SD and NC limit states are more evident in buildings with five stories high, due to their greater ductility.

5.3. Seismic Vulnerability Functions for Risk Analysis

The seismic vulnerability functions used for the economic risk assessment were derived by convolving the previous seismic fragility curves with the cumulative cost of a given damage state (damage to loss).

To estimate the physical damage and the respective economic losses, each limit state (LS) was assigned to the non-dimensional parameter variable damage ratio (DR), which represents the ratio between repair cost to the replacement cost involved in the occurrence of physical damage, allowing to

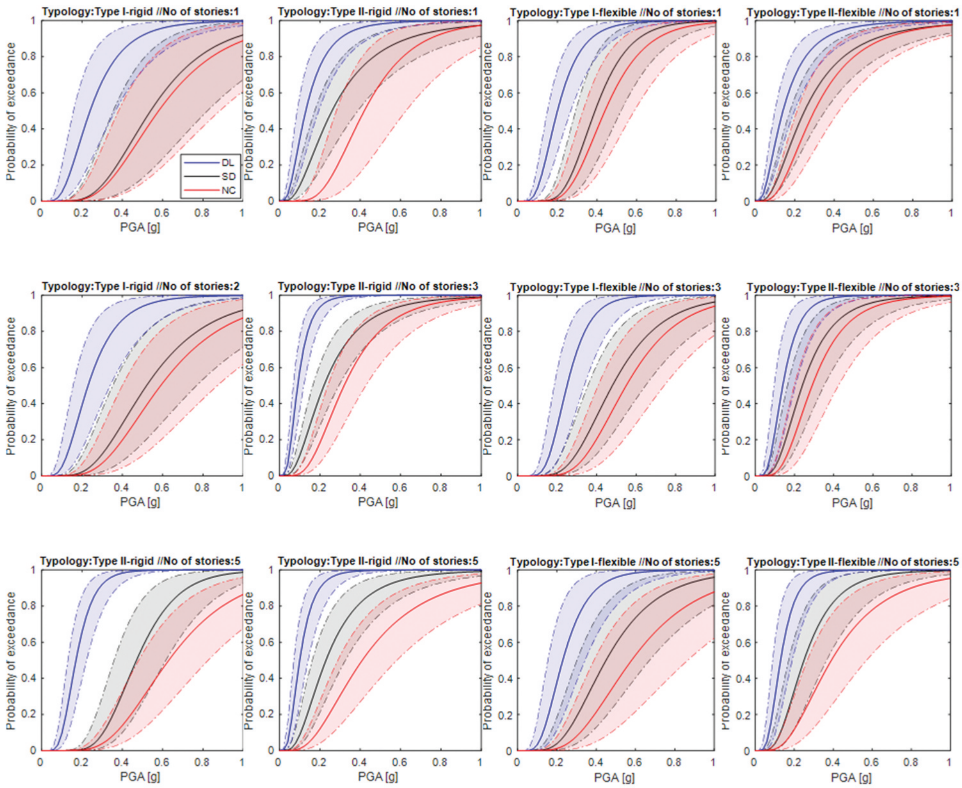

Figure 9. Seismic fragility curves for the LS adopted (DL, SD and NC) and buildings with one, three and five stories high (rigid and flexible floors).

Table 2. Assignment of damage ratio to the limit states adopted.

Damage grade (EMS-98)	Limit states adopted	Damage ratio (%)
Grade 1: Negligible to slight damage (no structural damage, non-structural damage)	–	0
Grade 2: Moderate damage (slight structural damage, moderate non-structural damage)	Damage limitation (DL)	15
Grade 3: Substantial to heavy damage (moderate structural damage, heavy non-structural)	Significant damage (SD)	50
Grade 4: Very heavy damage (heavy structural damage, very heavy non-structural damage)	Near collapse (NC)	100
Grade 5: Destruction (very heavy structural damage)	–	100

convert the damage level into financial losses. In the literature, several authors provide different economic loss indicators based on expert judgment or empirical post-earthquake studies of loss data. A review of the cost ratios assigned to damage states can be found in Hill and Rossetto (Hill and Rossetto 2008).

For the present work, the DR was assigned to the damage grades proposed in the EMS-98. The link between the limit states adopted in this study and those suggested by the EMS-98 was also discussed in Bernardo et al. 2022. Table 2 summarizes the damage ratio considered for the DL, SD, and NC limit states.

The damage vulnerability curves shown in Fig. 10 were computed for each building typology and different seismic intensity levels by summing the product of the percentage of exceedance of a given limit state (see Fig. 9) with the corresponding DR prescribed in Table 2. Analyzing Fig. 10, it can be seen that there are slight differences among numbers of floors and that damageability is higher for Type II typology (low-quality material), in particular for flexible floors.

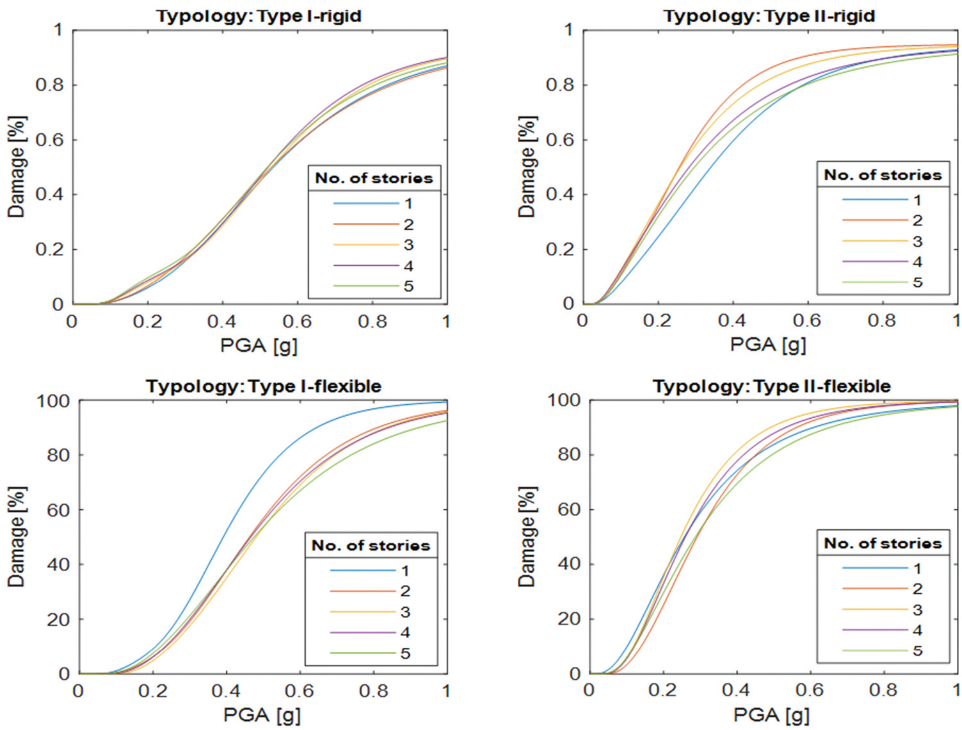

Figure 10. Damage vulnerability functions for different typologies and number of stories.

6. Seismic Risk Assessment in the MAL Region

The seismic risk curves presented in this section were computed in terms of economic losses, converting the lost building area to monetary value. For this purpose, the damage vulnerability functions presented in Fig. 10 were normalized by the total floor area of the buildings, considering different number of stories, resulting in a unique equivalent lost area function disaggregated per typological class, as depicted in Fig. 11a. The results are shown in terms of the return period associated with the seismic scenario. The expected losses conditioned by a seismic hazard level can be computed from the product of the respective equivalent lost area function by the replacement cost per square

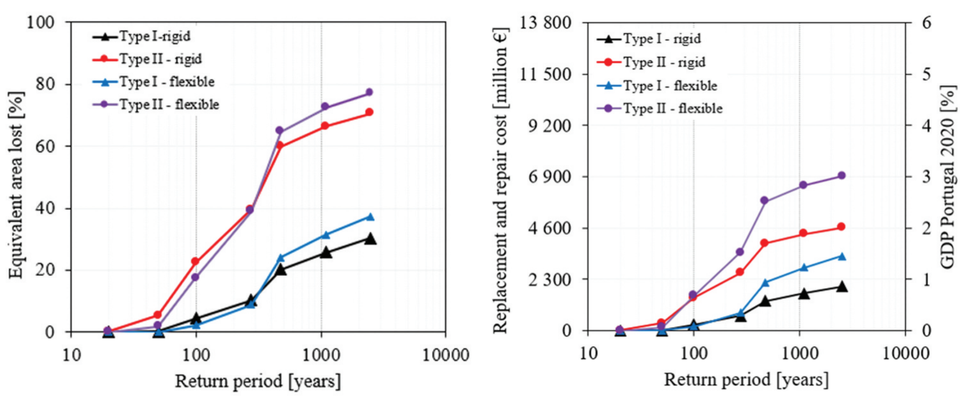

Figure 11. Disaggregation of the losses by typology of pre-code masonry buildings in the MAL region: (a) time-based variation of equivalent are lost; (b) seismic risk curves.

meter. Note that the results presented were computed for the corresponding exposure of each building class in order to achieve the equivalent lost area per typology. As can be noticed in Fig. 11a, the values of losses in buildings with flexible floors are slightly lower than those for rigid floors, until reaching, approximately, 275-years return period (RP); however, the opposite is verified for larger RP. This fact may be related to the higher ductility capacity of buildings with rigid floors and the damage propagation, i.e. although the damage seems to occur earlier in the case of buildings with rigid floors, when compared to flexible floors and lower seismic intensity levels, the former reach slightly lower damage values for moderate-to-high seismic intensity levels. This observation is clarified in Figs. 9 and 10.

Figure 11b presents the seismic risk curves for the different pre-code typologies analyzed, considering a replacement and repair cost equal to 828,48 €/m^2 and a total floor area of 789 ha and 1084 ha for rigid and flexible floors, respectively. From the analysis of this figure, it can be concluded that buildings with flexible floor diaphragms represent the largest economic losses in the MAL region. Note that, the losses in buildings with flexible floors are higher than in rigid floors (Fig. 11a), and their economic exposure is also higher, namely for Type II typology.

For instance, considering 10% probability of exceedance in 50 years (475–year return period), the values of area lost in Type II typology are about three times the values in Type I typology (Fig. 11a). Regarding the replacement and repair cost, it varies from 0.5% to 1.5% (rigid floors) and 0.75% to 2.3% (flexible floors) of the GDP in Portugal in 2020, assuming the total building stock composed by structures in good (Type I) or poor (Type II) state of conservation, respectively.

Finally, looking at the economic exposure of the pre-code masonry building stock, Fig. 12a,b show the grand total in terms of lost area and associated monetary value, respectively, considering different states of conservation/degradation: Type I (good state), Type II (poor state), and Type I/II by combining Type I and Type II. This stratification was based on the data provided by Census 2011 (INE 2012) regarding the state of conservation of the building stock in the MAL region. According to this information, 30% of the buildings are deemed to be in a poor state of conservation (Type II). Thus, the grand total was estimated for all building stock assuming these three states of conservation. By weighting Type I/II typologies according to their state of conservation, the economic loss was estimated at around 2.1% of GDP (2020) for a 475-years return period. For all building stock in good or poor state of conservation, the GDP loss values vary, approximately, between 1.5% (Type I) and 4.2% (Type II). Comparing these results with the literature, as validation against earthquake response data for such buildings is unavailable, Costa et al. (2010) estimated the economic loss for pre-code masonry buildings in the MAL region, achieving a loss value of around 1.9% of GDP (2001).

The previous results were also disaggregated by parishes, considering buildings with rigid (Fig. 13a) and flexible floors (Fig. 13b) separately and assuming the abovementioned weighting of 70% and 30% for Type I and Type II, respectively. Figure 13c shows the grand total in the MAL region by summing

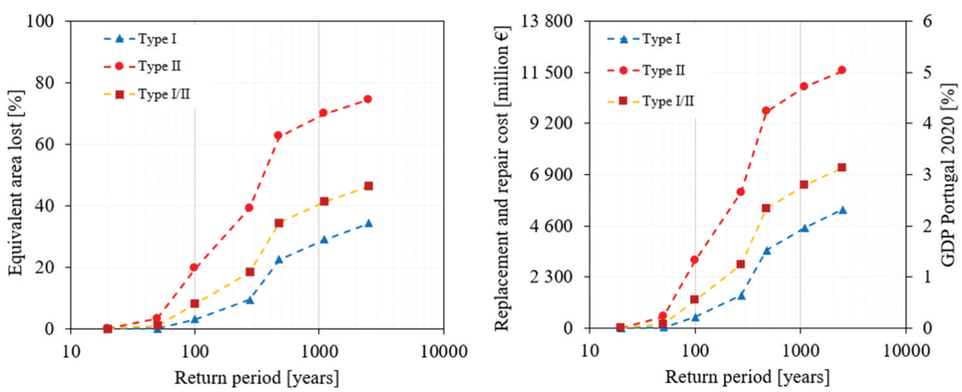

Figure 12. Grand total for the pre-code masonry building stock in the MAL region considering different states of conservation/degradation: (a) time-based variation of equivalent area lost; (b) seismic risk curves.

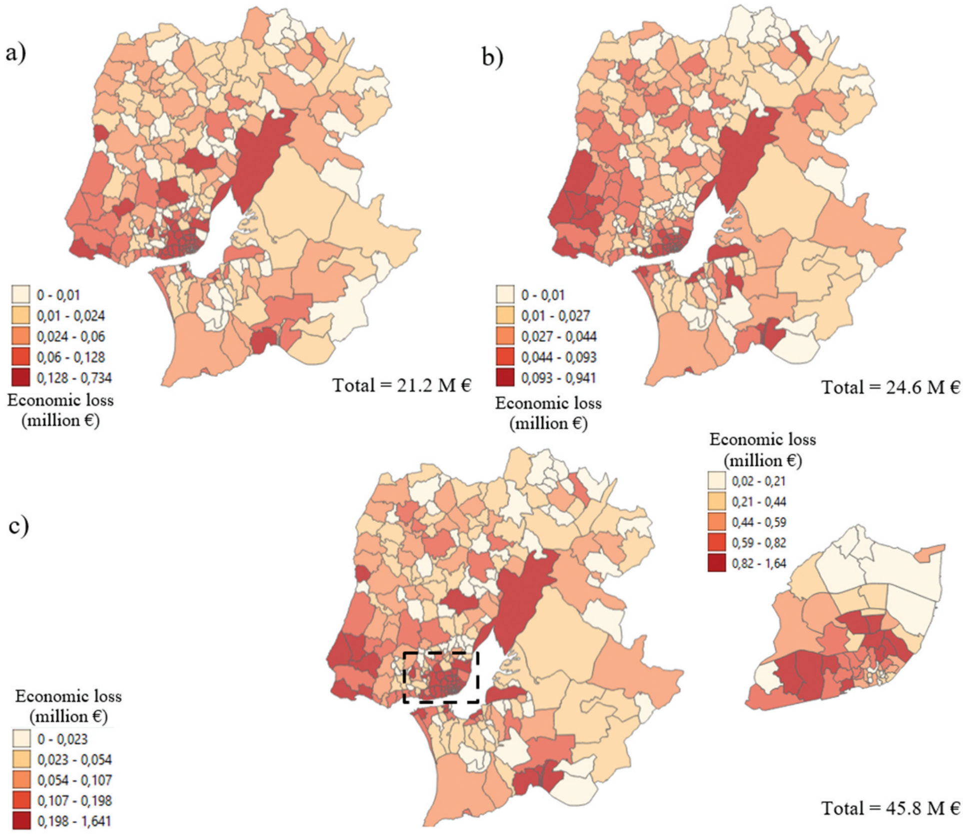

Figure 13. Annual expected losses (AEL) of the seismic risk in MAL for pre-code masonry buildings: (a) rigid floors (70% type I + 30% type II); (b) flexible floors (70% type I + 30% type II); (c) grand totals in the MAL region and in the Lisbon city center.

all buildings weighted. The values presented correspond to the annual expected losses (AEL) computed by combining the losses from all stochastic events, i.e. the sum of the products between the event annual rate and the associated losses. It should be noted that, since it was not considered the spatial variability of the seismic action, all parishes were assumed to be exposed to the same seismic intensity level; therefore, the differences of monetary values between parishes essentially reflect the economic exposure of each parish and the vulnerability of the typological class located in that region subjected to the same seismicity level.

Table 3 summarizes the annual expected loss (AEL) in the MAL region. Assuming independent events, the expected losses were also estimated for a lifetime period of 50 years. Looking at the grand total, the AEL of the equivalent area lost is around 0.30%, which corresponds to a monetary value of

Table 3. Summary of the economic risk of AEL and the investigation period of 50 years.

Economic risk	Type I rigid	Type II rigid	Type I flexible	Type II flexible	Rigid floors	Flexible floors	Grand total
Lost area [%]	0.16	0.70	0.15	0.59	0.32	0.28	0.30 (0.16 to 0.64)
AEL [€ x 10^6]	10.7	45.8	13.6	50.3	21.2	24.6	45.8
AEL/PIB 2020 [‰]	0.05	0.20	0.06	0.22	0.10	0.11	0.20
EL (50 years) [€ x 10^6]	512.9	1,934.6	652.6	2,195.7	939.4	1,115.5	2,504.9
EL (50 years)/PIB [‰]	2.23	8.41	2.84	9.55	4.08	4.85	8.94

45.8 M €. For the other states of conservation, the annual lost area expected may range from 0.16 (Type I) to 0.64 (Type II), respectively, 24.3 M € and 96.1 M €.

Sousa, Campos Costa, and Caldeira (2010) estimated AEL in the center of Lisbon at around 59.8 M €, for a short-distance seismic scenario. The AEL (grand total) estimated in the present study for the same region is approximately 29.4 M € (70% Type I + 30% Type II). Note that the values obtained in the present work are quite lower, since the study carried out by Sousa, Campos Costa, and Caldeira (2010) includes the entire building stock up to 2001, which naturally results in a higher exposure.

7. Final Comments and Conclusions

This work investigated the seismic risk in the parishes of the metropolitan area of Lisbon (MAL) region, forecasting the economic losses of masonry buildings built before the enforcement of the first seismic-code in 1958 in Portugal (RSCCS 1958). The study employs different typological class representative of the state of conservation/degradation of the building stock – Type I (good state of conservation) and Type II (poor state of conservation), both with rigid and flexible diaphragm floors.

The economic risk was evaluated through a probabilistic approach for the seismic scenario corresponding to the onshore source area of Lower Tagus Valley Fault (LTVF), which is the worst scenario for the region under study (Sousa 2006b). The economic exposure and the state of conservation of the building stock were based on the 2011 census (INE 2012). These data are still being used, since the new data from Census 2021 did not include the variable building typology in the survey. The capacity of the buildings and its dispersion were extracted from a previous work conducted by the authors (Bernardo, Campos Costa, et al. 2021). Based on such results, the seismic performance and associated variability due to stochastic realizations of the seismic scenario were here computed over a wide range of Mw. It is also important to stress that some simplifications have been considered in the study, namely the computation of uniform seismic ground motions in the entire region (given the short source-to-site distance), at bedrock level, since it represents the vast majority of site conditions in the MAL region (Costa et al. 2010).

The economic seismic risk of the MAL region, evaluated in terms of the replacement cost of the residential building stock in good state of conservation (Type I), varies from 0.2% to 2.3% GDP (2020), corresponding to a percentage of area lost between 3% and 34%, for 100- to 2500-years return period (RP), respectively. Considering a poor state of conservation of the entire building stock, the values of economic losses in terms of GDP ratio can reach 1.3% (100-years RP) and 5.0% (2500-years RP), resulting in about 19.5% to 74.5% of area lost, respectively. For an intermediate state of conservation (30% Type I and 70% Type II), the estimated losses vary from 0.5% to 3.1% for the abovementioned RP. Furthermore, the greatest risk is due to buildings with flexible floor diaphragms given their higher exposure in the MAL region.

AEL for the entire pre-code masonry building stock in the MAL region results in a monetary value of 45.8 M €, whereas 2,504.9 M € loss was found for a lifetime period of 50 years, considering for both an intermediate state conservation. From the disaggregation of the seismic risk by parishes, it can be concluded that the regions of downtown Lisbon, Sintra, Cascais, Setúbal, Montijo, Almada, and Vila Franca de Xira should be prioritized for earthquake mitigation measures and emergency plans, given the high exposure of pre-code masonry buildings, namely the ones with flexible floors which are more vulnerable to moderate and high seismic intensities.

Despite the contribution of the study in providing valuable information to support building owners and risk management decision-making, it is important to note that the results and conclusions were obtained without considering the out-of-plane behaviors of the masonry walls and local soil conditions. Further studies should be conducted to evaluate the effects of soil amplification at the surface on building performance. Nevertheless, the methodology can be applied to other typologies following a similar probabilistic framework, which should include geometry surveys to derive representative structures, and extended to the estimation of indirect losses, providing a holistic risk assessment of the region.

Disclosure Statement

No potential conflict of interest was reported by the author(s).

Funding

This work was supported by the Foundation for Science and Technology (FCT) under Grant number PD/BD/135325/2017 in the scope of the InfraRisk Doctoral Programme – Analysis and Mitigation of Risks in Infrastructures.

ORCID

V. Bernardo http://orcid.org/0000-0002-5071-8155
A. Campos Costa http://orcid.org/0000-0001-6869-9186
P. Candeias http://orcid.org/0000-0003-4873-7979
A. Costa http://orcid.org/0000-0001-8950-4843

References

Barbat, A. H., L. G. Pujades, and N. Lantada. 2008. "Seismic Damage Evaluation in Urban Areas Using the Capacity Spectrum Method: Application to Barcelona." *Soil Dynamics and Earthquake Engineering* 28 (10–11): 851–865. https://doi.org/10.1016/j.soildyn.2007.10.006.

Battegazzorre, E., A. Bottino, M. Domaneschi, and G. P. Cimellaro. 2021. "IdealCity: A Hybrid Approach to Seismic Evacuation Modeling." *Advances in Engineering Software* 153:102956. https://doi.org/10.1016/j.advengsoft.2020.102956.

Beresnev, I. A., and G. M. Atkinson. 1998. "FINSIM - A FORTRAN Program for Simulating Stochastic Acceleration Time Histories from Finite Faults." *Seismological Research Letters* 69 (1): 27–32. https://doi.org/10.1785/gssrl.69.1.27.

Bernardo, V., A. Campos Costa, P. Candeias, and A. Costa. 2021. "Seismic Vulnerability Assessment and Fragility Analysis of Pre-Code Masonry Buildings in Portugal." *Bulletin of Earthquake Engineering*. https://doi.org/10.1007/s10518-022-01434-8.

Bernardo, V., A. Campos Costa, P. Candeias, A. Costa, A. Marques, and A. Carvalho. 2022. "Ambient Vibration Testing and Seismic Fragility Analysis of Masonry Building Aggregates." *Bulletin of Earthquake Engineering* [Internet] 20 (10): 5047–5071. https://doi.org/10.1007/s10518-022-01387-y.

Bernardo, V., R. Sousa, P. Candeias, A. Costa, and C. A. Campos. 2021. "Historic Appraisal Review and Geometric Characterization of Old Masonry Buildings in Lisbon for Seismic Risk Assessment." *International Journal of Architectural Heritage* 16 (12): 1921–1941. https://doi.org/10.1080/15583058.2021.1918287.

Campos Costa, A., M. L. Sousa, A. Carvalho, and E. Coelho. 2006. "Seismic Loss Scenarios Based on Hazard Disaggregation. Application to the Metropolitan Region of Lisbon, Portugal." *Assessing and Managing Earthquake Risk*.

Candeias, P., A. Correia, A. C. Costa, J. M. Catarino, M. Pipa, H. Cruz, E. Carvalho, and A. Costa. 2020. "General Aspects of the Application in Portugal of Eurocode 8 – Part 3 – Annex C (Informative) – Masonry Buildings [In Portuguese]." *Revista Portuguesa de Engenharia de Estruturas* 12.

Carvalho, A., G. Zonno, G. Franceschina, J. Bilé Serra, and A. Campos Costa. 2008. "Earthquake Shaking Scenarios for the Metropolitan Area of Lisbon." *Soil Dynamics and Earthquake Engineering* 28 (5): 347–364. https://doi.org/10.1016/j.soildyn.2007.07.009.

Choffat, P., and A. Bensaúde. 1912. *Estudos sobre o sismo do Ribatejo de 23 de Abril de 1909*. Lisbon, Portugal: Imprensa Nacional. [in Portuguese].

Correia, M. R., P. B. Lourenço, and H. Varum. 2015. *Seismic Retrofitting: Learning from Vernacular Architecture*. 1st ed. Taylor & Francis, editor. CRC Press.

Costa, A. C., M. L. Sousa, A. Carvalho, and E. Coelho. 2010. "Evaluation of Seismic Risk and Mitigation Strategies for the Existing Building Stock: Application of LNECloss to the Metropolitan Area of Lisbon." *Bulletin of Earthquake Engineering* 8 (1): 119–134. https://doi.org/10.1007/s10518-009-9160-3.

Crowley, H., J. Dabbeek, V. Despotaki, D. Rodrigues, L. Martins, V. Silva, X. Romão, N. Pereira, G. Weatherill, and L. Danciu. 2021. *European Seismic Risk Model (ESRM20). V1.0.1*. Pavia: Eucentre.

Crowley, H., R. Pinho, M. Pagani, and N. Keller. 2013. "Assessing Global Earthquake Risks: The Global Earthquake Model (GEM) Initiative." *Handbook of Seismic Risk Analysis and Management of Civil Infrastructure Systems*. https://doi.org/10.1533/9780857098986.5.815.

D'Ayala, D. 2013. *Assessing the Seismic Vulnerability of Masonry Buildings*. Edited by S. Tesfamariam and K. Goda. Woodhead Publishing Limited. https://doi.org/10.1533/9780857098986.3.334.

De Iuliis, M., E. Battegazzorre, M. Domaneschi, G. P. Cimellaro, and A. G. Bottino. 2023. Large Scale Simulation of Pedestrian Seismic Evacuation Including Panic Behavior. Sustainable Cities and Society. https://doi.org/10.1016/j.scs.2023.104527.

Domaneschi, M., G. P. Cimellaro, and G. Scutiero. 2019. "A Simplified Method to Assess Generation of Seismic Debris for Masonry Structures." *Engineering Structures* 186:306–320. https://doi.org/10.1016/j.engstruct.2019.01.092.

Domaneschi, M., A. Zamani Noori, M. V. Pietropinto, and G. P. Cimellaro. 2021. *Seismic Vulnerability Assessment of Existing School Buildings*. Computers and Structures. https://doi.org/10.1016/j.compstruc.2021.106522.

Douglas, J., D. M. Seyedi, T. Ulrich, H. Modaressi, E. Foerster, K. Pitilakis, D. Pitilakis, et al. 2015. "Evaluation of Seismic Hazard for the Assessment of Historical Elements at Risk: Description of Input and Selection of Intensity Measures." *Bulletin of Earthquake Engineering* 13 (1): 49–65. https://doi.org/10.1007/s10518-014-9606-0.

FEMA. 2005. *Improvement of Nonlinear Static Seismic Analysis Procedures. FEMA 440*. Washington DC: Federal Emergency Management Agency.

Ferreira, T. M., R. Vicente, J. A. R. Mendes da Silva, H. Varum, and A. Costa. 2013. "Seismic Vulnerability Assessment of Historical Urban Centres: Case Study of the Old City Centre in Seixal, Portugal." *Bulletin of Earthquake Engineering* 11 (5): 1753–1773. https://doi.org/10.1007/s10518-013-9447-2.

Flesch, R. 2007. "Lessloss: Risk Mitigation for Earthquakes and Landslides." In *European Manual for in-Situ Assessment of Important Existing Structures*, 1–182. Pavia, Italy: IUSS Press.

Foerster, E., Y. Krien, M. Dandoulaki, S. Priest, S. Tapsell, G. Delmonaco, C. Margottini, and C. Bonadonna. 2009. "WP 1: State-of-the-Art on Vulnerability Types: Methodologies to Assess Vulnerability of Structural Systems."

Hill, M. P., and T. Rossetto. 2008. "Do Existing Damage Scales Meet the Needs of Seismic Loss Estimation?" *The 14th World Conference on Earthquake Engineering*, Beijing, China.

INE. 2012. "Censos 2011 Resultados Definitivos. Report." Lisbon, Portugal [in Portuguese].

Lagomarsino, S., and S. Cattari. 2015. "PERPETUATE Guidelines for Seismic Performance-Based Assessment of Cultural Heritage Masonry Structures." *Bulletin of Earthquake Engineering* 13 (1): 13–47. https://doi.org/10.1007/s10518-014-9674-1.

Marasco, S., A. Cardoni, A. Zamani Noori, O. Kammouh, M. Domaneschi, and G. P. Cimellarof. 2021. "Integrated Platform to Assess Seismic Resilience at the Community Level. Sustainable Cities and Society." *Sustainable Cities and Society* 64:102506. https://doi.org/10.1016/j.scs.2020.102506.

Marasco, S., A. Z. Noori, M. Domaneschi, and G. P. Cimellaro. 2021. "Seismic Vulnerability Assessment Indices for Buildings: Proposals, Comparisons and Methodologies at Collapse Limit States." *International Journal of Disaster Risk Reduction* 63:102466. https://doi.org/10.1016/j.ijdrr.2021.102466.

Marasco, S., A. Zamani Noori, M. Domaneschi, and G. P. Cimellaro. 2021. A Computational Framework for Large-Scale Seismic Simulations of Residential Building Stock. *Engineering Structures*. https://doi.org/10.1016/j.engstruct.2021.112690.

Martins, L., and V. Silva. 2021. "Development of a Fragility and Vulnerability Model for Global Seismic Risk Analyses." *Bulletin of Earthquake Engineering* 19 (15): 6719–6745. https://doi.org/10.1007/s10518-020-00885-1.

McGuire, R. K. 2004. *MNO-10, Seismic Hazard and Risk Analysis*. Earthquake Engineering Research Institute.

Milosevic, J. 2019. "Seismic Vulnerability Assessment of Mixed Masonry-Reinforced Concrete Buildings in Lisbon." PhD Thesis, Technical University of Lisbon, Lisbon, Portugal [in Portuguese].

Milosevic, J., S. Cattari, and R. Bento. 2020. "Definition of Fragility Curves Through Nonlinear Static Analyses: Procedure and Application to a Mixed Masonry-RC Building Stock." *Bulletin of Earthquake Engineering* 18 (2): 513–545. https://doi.org/10.1007/s10518-019-00694-1.

Mouroux, P., and B. Le Brun. 2006. "Presentation of RISK-UE Project." *Bulletin of Earthquake Engineering* 4 (4): 323–339. https://doi.org/10.1007/s10518-006-9020-3.

Penna, A., S. Lagomarsino, and A. Galasco. 2014. "A Nonlinear Macroelement Model for the Seismic Analysis of Masonry Buildings." *Earthquake Engineering & Structural Dynamics* 43 (2): 159–179. https://doi.org/10.1002/eqe.2335.

Pereira, N., and X. Romao. 2016. Seismic Resistance of Portuguese Vernacular Architecture: A Critical Review. Report [Internet]. Porto: University of Porto. http://www.ceru-europa.pt.

Rojahn, C., R. L. Sharpe, R. E. Scholl, A. S. Kiremidjian, and R. V. Nutt. 1985. *Earthquake Damage Evaluation Data for California*.

RSCCS. 1958. "National Standard: Code for Building Safety Against Earthquakes (Original Title: Regulamento de Segurança Das Construções Contra Os Sismos – RSCCS)."

Silva, V., H. Crowley, H. Varum, and R. Pinho. 2014. "Seismic Risk Assessment for Mainland Portugal." *Bulletin of Earthquake Engineering* 13 (2): 429–457. https://doi.org/10.1007/s10518-014-9630-0.

Silva, V., M. Pagani, J. Schneider, and P. Henshaw. 2018. "Assessing Seismic Hazard and Risk Globally for an Earthquake Resilient World."

Simões, A. G., R. Bento, S. Lagomarsino, S. Cattari, and P. B. Lourenço. 2020. "Seismic Assessment of Nineteenth and Twentieth Centuries URM Buildings in Lisbon: Structural Features and Derivation of Fragility Curves." *Bulletin of Earthquake Engineering* [Internet] 18 (2): 645–672. https://doi.org/10.1007/s10518-019-00618-z.

Simões, A. G. G. 2018. "Evaluation of the Seismic Vulnerability of the Unreinforced Masonry Buildings Constructed in the Transition Between the 19th and 20th Centuries in Lisbon." PhD Thesis, Technical University of Lisbon, Lisbon, Portugal [in Portuguese].

Sousa, M. L. 2006a. "Risco Sísmico em Portugal Continental."

Sousa, M. L. 2006b. "Seismic Risk in Mainland Portugal." PhD Thesis, Technical University of Lisbon, Lisbon, Portugal [in Portuguese].

Sousa, M. L., A. Campos Costa, and L. Caldeira. 2010. "Seismic Risk Assessment in Lisbon."

Tang, Y., Y. Yin, K. Hill, V. Katiyar, A. Nasseri, and T. Lai. 2012. "Seismic Risk Assessment of Lisbon Metropolitan Area Under a Recurrence of the 1755 Earthquake with Tsunami Inundation." *15th World Conference on Earthquake Engineering (15WCEE)*, Lisbon, Portugal [in Portuguese]. Geology, Environmental Science.

Vamvatsikos, D. 2013. "Derivation of New SAC/FEMA Performance Evaluation Solutions with Second-Order Hazard Approximation." *Earthquake Engineering & Structural Dynamics* [Internet] 42 (8): 1171–1188. https://doi.org/10.1002/eqe.2265.

Vicente, R., T. Ferreira, and R. Maio. 2014. *Seismic Risk at the Urban Scale: Assessment, Mapping and Planning*. Procedia Economics and Finance. https://doi.org/10.1016/S2212-5671(14)00915-0.

Vicente, R., S. Parodi, S. Lagomarsino, H. Varum, and J. Silva. 2011. "Seismic Vulnerability and Risk Assessment: Case Study of the Historic City Centre of Coimbra, Portugal." *Bulletin of Earthquake Engineering* 9 (4): 1067–1096. https://doi.org/10.1007/s10518-010-9233-3.

Vilanova, S. P., and J. F. B. D. Fonseca. 2007. "Probabilistic Seismic-Hazard Assessment for Portugal. Bulletin of the Seismological Society of America." *Bulletin of the Seismological Society of America* 97 (5): 1702–1717. https://doi.org/10.1785/0120050198.